

## Nano-magnetite; Optimization and Characterization

A. Elfalaky\*, S. Soliman and H. Elmosallamy

Department of Physics, Faculty of Science, Zagazig University, Zagazig, Egypt

---

**Abstract:** Nanoparticles of magnetite were synthesized using aqueous chlorides solutions via coprecipitation technique. The structure and crystallite size of the precipitate were inspected and analyzed regarding X-ray diffraction. Cation distribution of magnetite of the form  $(Fe^{3+}_{(2-x)} Fe^{2+}_y) (Fe^{2+}_{(1-y)} Fe^{3+}_x)$  has been proved and optimized where the cation parameters  $x$  and  $y$  were determined using the experimental value of magnetite magnetic moment. Spin-Orbit coupling calculations based on density functional theory were applied. Full optimization was considered and the most stable configuration was proffered. The density of states of magnetite was calculated. The inclination of half metallicity of magnetite was scrutinized. DC electrical resistance of pressed disk shape magnetite nanoparticles was measured at room and elevated temperatures. The results are discussed and analyzed in terms of DOS and cation distribution.

**Key Words:** Half metallic, Magnetite, Electrical resistance, Nano-crystals, DOS.

---

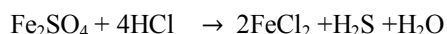
### I. Introduction

Spinel ferrites are group of materials that have distinctive flexible structure, according to which the characteristics are adopted. Ferrite structure was established and recognized to be close packed array of oxide anions with two interstitial cation sites A (tetrahedral) and B (octahedral) sublattices with chemical formula  $AB_2O_4$  [1]. A and B are divalent and trivalent elements respectively. The proper elemental selection and occupancy of these sites drastically modify the corresponding physical property. Such modification is attributed to the surroundings generated crystal field. There are three configurations for the ferrite cation distribution; normal, inverse and mixed spinels. General formula for the mixed spinel ferrite of the form  $(A_y B_{(2-x)}) [A_{(1-y)} B_x]$  has been figured out and according to the values of  $x$  and  $y$  the spinel is said to be normal, mixed or inverse spinel. In addition, the parameters  $x$  and  $y$ , of the cation distribution, play an active part in adopting the physical properties of ferrites. Hence the aspect of applications might also be strongly influenced by these parameters. Many investigations have been devoted for estimating  $x$  and  $y$ . Magnetite, the chemical formula of which is  $Fe_3O_4$ , is well known for quite long time ago. It has an interesting characteristics and it is the subject of quite large number of publications since the forty of the last century [2-4]. Recently magnetite has been involved in the nanoparticle applications and the spintronic field of research [5-7]. It has been theoretically confirmed that magnetite is a ferrimagnetic half metallic, HM, compound in which the density of states, DOS, overlaps the Fermi level for one spin channel while gap is created for the other spin channel. In accord magnetite has 100% spin polarization at the Fermi level. Besides, magnetite has low electrical resistivity at room temperature and has very high Curie temperature. Such unique features support magnetite to be functional magneto spintronic material [8-9].

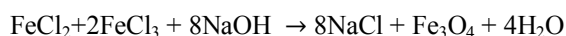
The objectives of this study are to investigate the crystallographic structure of nanoparticles magnetite, optimize the cation distribution of magnetite and correlate the experimental results of the electrical resistance with both the cation distribution and the DOS data.

### Experimental techniques and calculations

Nanoparticles of magnetite were prepared utilizing the coprecipitation technique.  $FeCl_2$  was first synthesized from iron sulfate according to the reaction:



Aqueous solutions of iron chlorides and NaOH were substitutionally reacted as follow:



Molar weights of the above constituents were dissolved in distilled water and thoroughly mixed using magnetic stirrer for 45 minutes. The pH and temperature of the medium were recorded and found to be 12 and 343 K respectively. The Black precipitate was washed and filtered several times until the precipitate is free of NaCl. The precipitate was air heated at 363 K for 6 hours to get rid of water.

Powder samples were X-ray examined utilizing Philips diffractometer (PW3040) with  $CuK_{\alpha 1}$  of wave length  $\lambda = 1.5406 \text{ \AA}$ . The crystallite size  $D$  of the prepared powder was calculated using two independent techniques, the X Powder [10] and Winfit [11] programs. Disk shaped samples were prepared by applying

hydraulic pressure about 5 ton/cm<sup>2</sup>. The resistance of disk shaped sample was measured against temperature over the temperature range (300 - 673 K) using two probe method.

Using Local augmented plane wave (LAPW) code Wien2k [12-13] the Spin-Orbit coupling calculations based on density functional theory were performed. In order to treat the high lying semicore states of Fe-3d states and to relax linearization errors Local orbitals were employed. Exchange correlation was taken within the generalized gradient approximation GGA. The energy threshold between the core and the valance states was set -6.8 Ry. The muffin tin-radii ( $R_{MT}$ ) were chosen to ensure nearly touching spheres and minimizing the interstitial space.

## II. Result and Discussions

### 1-Structural analysis:-

The structure of the synthesized magnetite has been identified using X-ray scattering. The diffraction pattern of the studied powder is shown in Fig (1). It is clear that, regarding the ICDD card, 89-0951, only single phase of the spinel ferrite is present and no secondary phases were detected. The corresponding crystal structure has been recognized to be FCC phase with an average lattice constant  $a_x = 8.3974 \text{ \AA}$  and  $\alpha = \beta = \gamma = 90^\circ$ . Such value of the lattice constant seems to be consistent with the previously reported values [9].

It can be easily noticed that the peaks of the diffraction pattern are broad indicating that the crystallites are of fine size. According to the data from X-ray apparatus the crystallite size corresponding to the most intense peak (311) is about 29.8 nm. The average crystallite size was estimated using Winfit program and found to be about 27 nm. An estimation of the crystallite size of magnetite using X Powder program for plane (311) is about 27.98 nm. Such values of crystallite size seem likely to be consistent.

### 2-Cation distribution optimization:

Magnetite has spinel structure with general formula  $AB_2O_4$  where the oxygen anions occupy the corners and the face centered of close-packed FCC. The cations A and B occupy the interstitial sites. Assuming the cation distribution of magnetite has general configuration of the form:  
 $(Fe^{3+}_{(2-x)} Fe^{2+}_y) \{Fe^{2+}_{(1-y)} Fe^{3+}_x\}$

where the ( ) represents the tetrahedral A site and { } denotes the octahedral B site. To optimize the cation distribution the cationic parameters X and y had to be calculated.

Since magnetite is ferrimagnetic material with magnetic moment about  $4.1 \mu_B$  and according to Hund's rule, the magnetic moment of Fe ( $3d^6 4s^2$ ) is  $4 \mu_B$ , that of  $Fe^{2+}$  ( $3d^6$ ) is  $4 \mu_B$  and that for  $Fe^{3+}$  ( $3d^5$ ) is  $5 \mu_B$ . Due to the existence of ions with different valence in the unit cell ( $Fe^{3+}$  &  $Fe^{2+}$ ) the octahedral Fe ions are antiferromagnetically coupled to those in tetrahedral bring along net magnetic moment. The magnetic moment per unit formula can be calculated according to the above cation distribution in such a way that the magnetic moment of the A site is given by  $m_A$ :

$$m_A = (2-X) \cdot M_{Fe3} + y \cdot M_{Fe2} \quad (1)$$

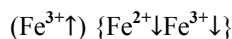
For the site B the magnetic moment is given by:

$$m_B = (1-X) \cdot M_{Fe3} + (1-y) \cdot M_{Fe2} \quad (2)$$

The magnetic moment per unit formula of magnetite, m, is given by:

$$m = m_B - m_A \quad (3)$$

where  $M_{Fe2}$  and  $M_{Fe3}$  are the magnetic moments of  $Fe^{2+}$  and  $Fe^{3+}$  ions respectively. The values of  $m_A$ ,  $m_B$  and m were calculated for various values of the parameters X and y. Figure (2) represents the variation of  $m_A$  and  $m_B$  against X for different y values. It can be seen that for any value of y the magnetic moment of the tetrahedral A site tends to decrease with the increase of the cation parameter X. While that for the octahedral B site tends to increase with X increasing. Fig.(3) plots the dependence of m, the total magnetic moment per formula unit, against parameter X for different values of y. The reported value of the magnetic moment,  $M_{ex}$ , of magnetite, which is  $4 \mu_B$ , is represented by horizontal straight line. The indices of the points of interception of the straight line, corresponding to  $M_{ex}$ , with y curves represent the values X and y to be substituted in the cation distribution formula. The optimum value of y is that gives lattice constant equal to or near from the experimental value. In other words the optimum cation parameters are that correspond to index (X, y) verifying the experimental data of lattice constant and the magnetic moment [14]. On that regard the optimum value of X is 1 and that of y is 0. Therefore the optimum cation distribution is of the form:



According to this cation distribution magnetite is an inverse ferrite where the tetrahedral A site contains only the  $\text{Fe}^{3+\uparrow}$  ions while the B site contains both  $\text{Fe}^{2+\downarrow}$  and  $\text{Fe}^{3+\downarrow}$  ions. The octahedral ions are ferromagnetically coupled through double-exchange. However the  $\text{Fe}^{3+}$  ions on (tetra and octa) are antiferromagnetically coupled within the super-exchange. Considering the site spin, as schematically shown in Fig.(4), the ultimate magnetic moment is  $4 \mu_B$ . Consequently the magnetization of magnetite is associated with unidirectional spin, the spin of  $\text{Fe}^{2+\downarrow}$  in the B sites, and it is a spin polarized. It has been confirmed that the electrical conduction in ferrites is contributed to the octahedral B site [15]. In accordance the conduction in magnetite is associated with the ions of the B site. The extra electron in the  $\text{Fe}^{2+\downarrow}$  ion, called itinerant electron, goes back and forth between  $\text{Fe}^{2+\downarrow}$  and  $\text{Fe}^{3+\downarrow}$  as illustrated in Fig.(5).

### 3- DC electrical resistance:

The DC electrical resistance  $R$  of pressed nanoparticles magnetite is measured against temperature in temperature range from 300K up to 700K and the results of which are represented in Fig. (6). It can be seen that the resistance shows sharp decrease from about 42 M $\Omega$  at 300K to 0.2M $\Omega$  at 470K. Afterwards the resistance behaves independently of temperature up to 700K. Such anomaly has been observed before [16-17]. Such trend does not relate either to the metallic trend or to the semiconducting one. It is well known that  $R$  at such high temperature is dominated by the phonon interaction contribution. Which means that  $R \propto T^n$ , where  $n$  is either negative for semiconductors or positive for metals and conductors. It is well known that the conduction mechanism in magnetite, as in most ferrites, is due to hopping conduction. For the above suggested cation distribution, the hopping takes place between  $\text{Fe}^{2+\downarrow}$  and  $\text{Fe}^{3+\downarrow}$  ions within the octahedral B sites as schematically shown in Fig.(5). Accordingly the conduction through magnetite is due to hopping of the spin up electron between the two iron ions. Thus the conduction in magnetite is spin polarized. The temperature independence of  $R$  of magnetite can be attributed to the migration of  $\text{Fe}^{2+\downarrow}$  from the B sites to the A sites. Accordingly the increase of  $R$  due to phonon scattering is compensated with the decrease of concentration of  $\text{Fe}^{2+\downarrow}$  on the B sites. Therefore the resistance of magnetite tends to be temperature independent.

### III. Theoretical investigation

The electronic structure of magnetite was calculated using full optimization. Site symmetry, configurations of cation distribution, spin arrangement and oxygen positional parameter were considered in the optimization. Figure (7) represents the full optimization for lowest energy spin arrangement of magnetite. It has been found that the most stable crystal structure of magnetite at room temperature is FCC with lattice constant  $a_c = 8.41 \text{ \AA}$ . Such value of lattice constant is consistent with the above obtained experimental value  $a_c$ .

Calculations concerning DOS were carried out for the optimized structure of magnetite. Figure (8) depicts the total density of states of magnetite using GGA approach. The figure indicates that the up spin states at the Fermi level have zero value i.e.  $N(E_F) = 0$ . In addition small gap of about 0.2 eV is shown. On the other hand the down spin panel contains DOS at the Fermi level. Such trend of DOS at the Fermi level indicates the metallic nature of magnetite for the spin down panel. Consequently magnetite is considered as a half-metallic compound. One can also observe that the DOS at the Fermi level is associated with Fe-3d electrons in the octahedral B site beside very small DOS associated with O-2p electrons. Thus the conduction is exclusively associated with the double exchange between  $\text{Fe}^{2+\downarrow}$  and  $\text{Fe}^{3+\downarrow}$  ions through the O 2p anion. In consistent with the cation distribution magnetite is spin polarized half-metallic compound.

### IV. Conclusion:

Magnetite nanocrystals have been successfully synthesized using chemical coprecipitation technique. The X-ray structural analysis revealed that magnetite has face centered cubic with lattice constant equals 8.3974  $\text{\AA}$  and of average crystallite size equals 25 nm.

A cation distribution of the form  $(\text{Fe}^{3+}_{(2-x)} \text{Fe}^{2+}_y) \{ \text{Fe}^{2+}_{(1-y)} \text{Fe}^{3+}_x \}$  has been suggested. The optimum values of the cation parameters were found to be 0 and 1 and thus magnetite is certainly inverse spinel. The conduction mechanism in nanoparticles magnetite is a result of hopping of the itinerant electron between  $\text{Fe}^{2+\downarrow}$  and  $\text{Fe}^{3+\downarrow}$  ions on the octahedral B site through the oxygen anion.

Theoretical calculations based on GGA approach indicated that the minority DOS of magnetite overlaps with the Fermi level while the majority DOS includes energy gap of value 0.2 eV. Spin polarization at the Fermi level is 100%. Moreover spin polarized electrons are ascribed to the Fe-3d electrons in the octahedral B site. Such transition is attributed to the spin up electron. The calculations manifest the half metallicity trend. In accord it is evident that magnetite nanoparticles have the feasibility to be one of the spintronic materials.

### References:

- [1]. R. Valenzuela, Magnetic Ceramics, Cambridge Univer. Press (1994).
- [2]. E. J. W. Verwey, Nature, 144 (1939) 327.
- [3]. F. Walz, J. Phys. Cond. Mat., 14 (2002) R285.
- [4]. S. K. Park, T. Ishikawa, and Y. Tokura, Phys. Rev. B 58, 3717.
- [5]. J. Tang, M. Myers, K. A. Bosnick, L. E. Brus, J. Phys. Chem B, 107, 7501 (2003).
- [6]. K. Jordan, et al. Phys. Rev. B 74, 085416, (2006).
- [7]. R. Arras, L. Calmels and B. Warot-Fonrose, Appl. Phys. Letter, 100, 032403 (2012).
- [8]. R. Prakash, R. J. Choudhary, L. S. Sharath Chandra, N. Lakshmi, DM Phase, J of Phys, 19, 486212 (2007).
- [9]. M. Fonin, Yu. S. Dedkov, R. Pentcheva, U. Rudiger, G. Guntherodt, J of Phys, 19, 315217 (2007).
- [10]. <http://www.xpowder.com>
- [11]. Winfit 1.2.1, 1997, [www.geol.uni-erlangen.de](http://www.geol.uni-erlangen.de).
- [12]. Blaha, K. Schwarz, P. Sorantin, and S. B. Tricky, Comput. Phys. Commn. 59, 399 (1990).
- [13]. Blaha, K. Schwarz, M. G. K. H. D. Kvasnicka, and J. Luitz, WIEN2k, An Augmented Plane Wave + Local Orbitals Program for Calculating Crystal Properties Karlheinz Schwarz, Techn. Universitat Wien, wien Austria (2001).
- [14]. A. Elfalaky, Applied Physics A, Solids and Surfaces, 59 (4) 389 (1994).
- [15]. S. Todo, K. Siratori, S. Kimura, J. Phys. Soc. Jap. 64, 2118 (1995).
- [16]. M. Fonin, Yu. S. Dedkov, R. Pentcheva, U. Rudiger, G. Guntherodt, J of Phys, Condensed Matter, 19, 315217 (2007).
- [17]. N. N. Song, H. T. Yang, F. Y. Li, Z. A. Li, W. Han, X. Ren, Y. Luo, X. C. Wang, C. Q. Jin, X. Q. Zhang, Z. H. Cahng. J. Appl. Phys. 113, 184309 (2013).

### Figure captions:

- Fig.(1): X-ray diffraction pattern for magnetite nanoparticles.
- Fig.(2): Variation of site magnetic moment against X for different values of y.
- Fig.(3): Variation of total magnetic moment against X for different values of y.
- Fig.(4): Schematic representations of (A-B) super-exchange and (B-B) double-exchange.
- Fig.(5): Hopping of itinerant electron between  $Fe^{2+}\downarrow$  and  $Fe^{3+}\downarrow$  ions.
- Fig.(6): Variation of magnetite resistance R against temperature.
- Fig.(7): Potential energy optimization for magnetite.
- Fig.(8): Total density of states DOS for magnetite.

Fig.(1)

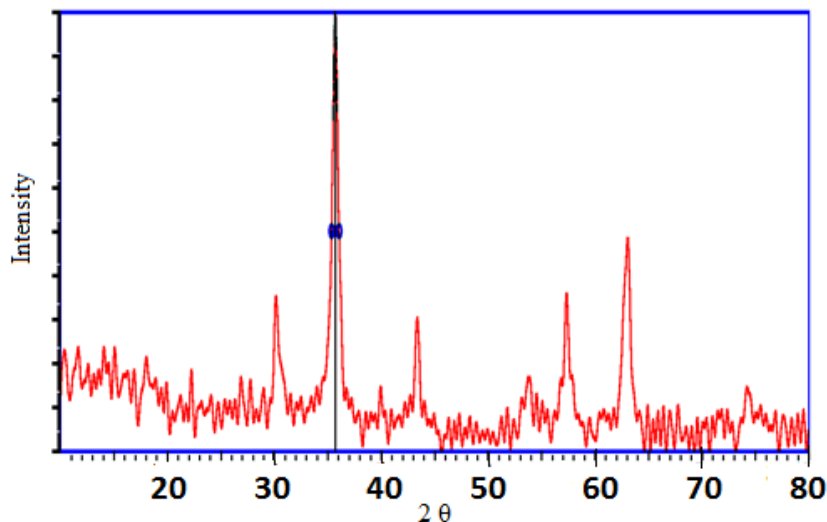


Fig.(2)

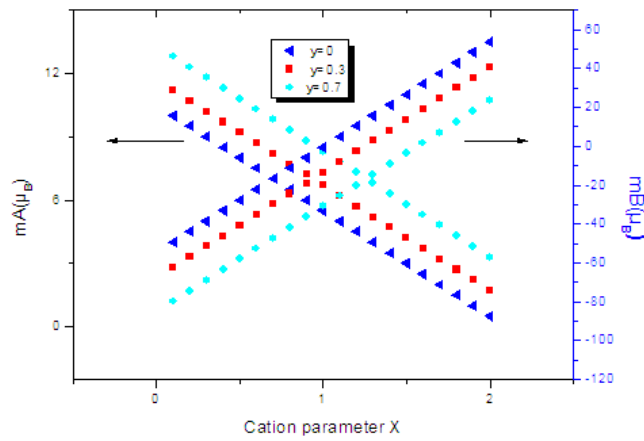


Fig.(3)

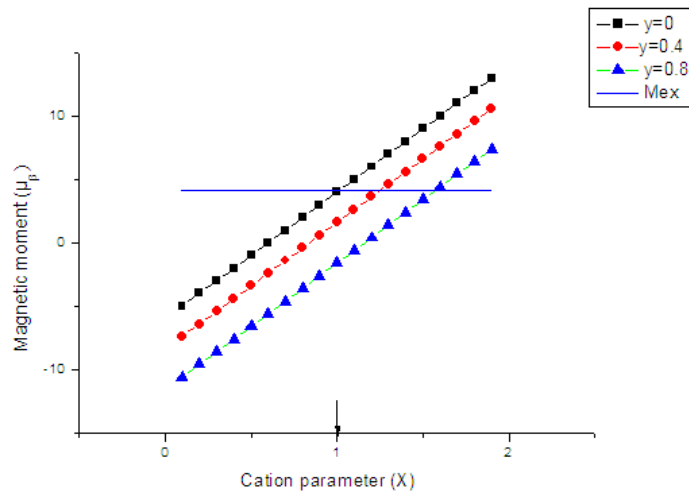


Fig.(4)

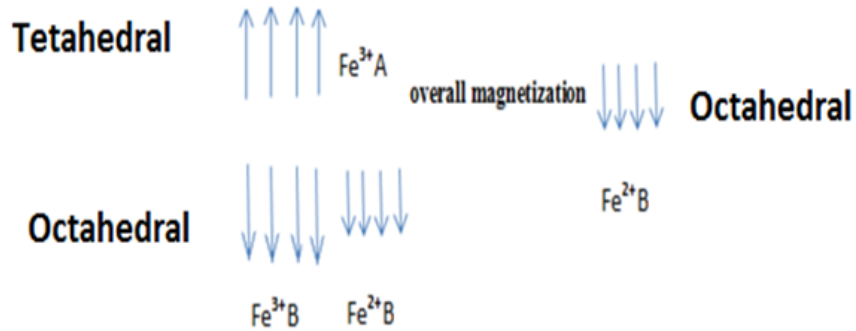


Fig.(5)

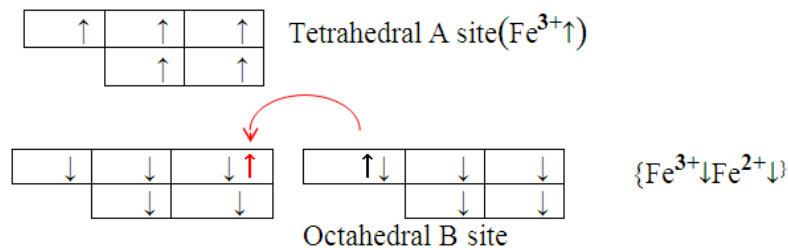


Fig.(6)

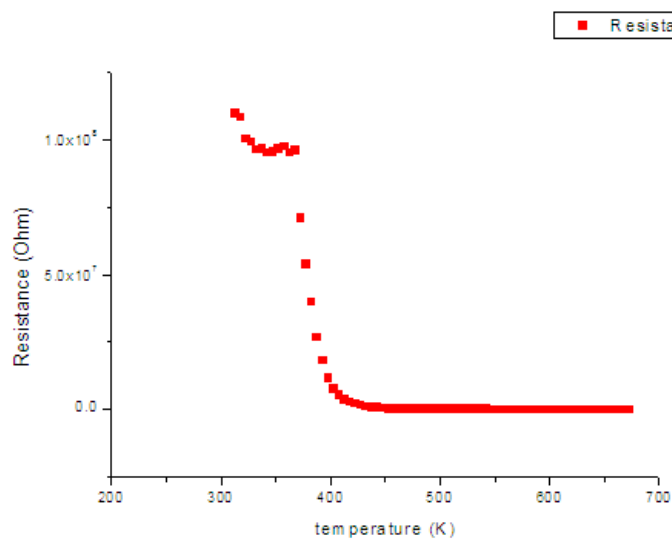


Fig.(7)

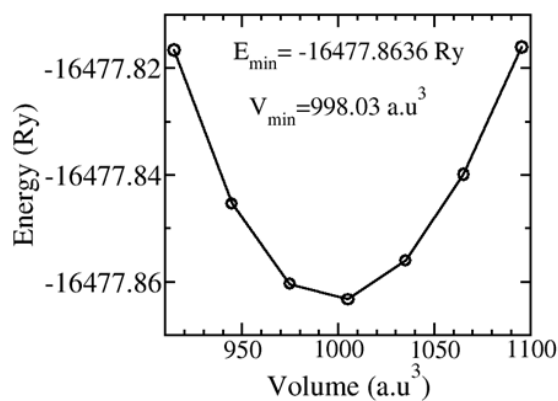


Fig.(8)

